Ultralow-temperature superplasticity and its novel mechanism in ultrafine-grained Al alloys

Nguyen Q. Chinh[1]*, Maxim Yu. Murashkin[2,3], Elena V. Bobruk[2,3], János L. Lábár[1], Jenő Gubicza[1], Zsolt Kovács[1], Anwar Q. Ahmed[1], Verena Maier-Kiener[4] and Ruslan Z. Valiev[2,3*]

[1]Department of Materials Physics, Eötvös Loránd University, 1-3 Egyetem tér, Budapest H-1053, Hungary

[2]Institute of Physics of Advanced Materials, Ufa State Aviation Technical University, 12 K. Marx St., Ufa 450008, Russia

[3]Laboratory for Mechanics of Bulk Nanomaterials, Saint Petersburg State University, 28 Universitetsky pr., Peterhof, St. Petersburg 198504, Russia

[4]Department of Physical Metallurgy and Materials Testing, Leoben University, 18 Franz Josef-Strasse, Leoben A-8700, Austria

*e-mails: chinh@metal.elte.hu, ruslan.valiev@ugatu.su

The important benefits of ultrafine-grained (UFG) alloys for various applications stem from their enhanced superplastic properties. However, decreasing the temperature of superplasticity and providing superplastic forming at lower temperatures and higher strain rates is still a priority. Here, we disclose the mechanism by which grain boundary sliding and rotation are enhanced, when UFG materials have grain boundary segregation of specific alloying elements. We present for the first time that such approach makes it possible to achieve superplasticity in conventional Al alloys at ultralow homologous temperatures below 0.5 (i.e., below 200 °C), which is important for developing new efficient technologies for manufacturing complex-shaped metallic parts with enhanced service properties, which are key factors for their applications.

1. Introduction

Superplasticity of materials is an important field of scientific research both because it presents significant challenges in the areas of flow mechanisms and because it forms the underlying basis for the commercial superplastic forming industry in which complex shapes and curved parts are formed from superplastic metals[1,2].

It is well established that two basic requirements must be fulfilled in order to achieve superplastic flow. First, superplasticity requires a very small grain size, typically smaller than ~10 μm. Second, superplasticity is a diffusion-controlled process operating with grain boundary sliding – as the main flow mechanisms - and therefore it requires a relatively high testing temperature typically at or above ~0.7 – 0.8 × T_m, where T_m is the absolute melting temperature of the material. At the same time, the developments of metallic materials during the last two decades with ultrafine grains of nanosized range by means of severe plastic deformation (SPD) processing paved the way towards new discoveries in the field of superplasticity[3,4]. Actually, the basic relationship for superplasticity has the form:

$$\dot{\varepsilon} = \frac{ADGb}{kT}\left(\frac{b}{d}\right)^q \left(\frac{\sigma}{G}\right)^{1/m}, \quad (1)$$

where $\dot{\varepsilon}$ is the strain rate of the deformation process, D is the appropriate diffusion coefficient, G is the shear modulus, b is the magnitude of the Burgers vector, k is Boltzmann's constant, T is the absolute temperature, d is the grain size, σ is the applied stress, q is the exponent of the inverse grain size, m is the strain rate sensitivity, and A is a dimensionless constant[1,2,5]. The temperature-dependence of the superplastic deformation is mainly determined by the diffusion coefficient, based on the formula

$$D = D_0 exp\left(\frac{-Q}{RT}\right), \quad (2)$$

where D_o is a frequency factor, Q is the activation energy, and R is the universal gas constant. Based on equation (1), the formation of ultrafine grains in the nanosized range provides an opportunity to control the temperature and the rate of superplastic flow in materials, which are

quite attractive for the practical application of their superplastic forming. In recent years, this problem was actively covered in literature[6–9]. Meanwhile, according to equations (1) and (2) the superplastic flow regimes may also be essentially controlled by diffusion. For UFG materials, it is the grain boundary diffusion associated with the development of grain boundary siding (GBS) and hence dependent on the structure of grain boundaries. In their turn, the recent precision studies of intergranular boundaries in UFG metals and alloys reveal that their grain boundaries have different defect structures and chemical compositions, depending on the SPD processing regimes[3,10,11]. This opens new opportunities in controlling the properties of superplastic materials.

In the present paper, this approach is for the first time investigated and demonstrated for an Al-Zn-Mg-Zr aluminum alloy. This widely used age-hardenable alloy of the Al-Zn-Mg (7xxx) series with multi-alloying elements was chosen due to fact that, it is the one of the basic materials in the aluminum industry. These alloys are generally used after conventional treatments and, as having an average grain size of 5-10 μm, they can be deformed superplastically for a total elongation of 300–500%, but only at high temperature of about 500 °C (~0.8 × T_m)[1,5]. The work presented here reports a unique grain boundary behavior controlled by relatively fast diffusion in an ultrafine-grained Al-Zn-Mg-Zr alloy, which can be deformed superplastically with a record total elongation of 500% in a temperature region lower than 170 °C (0.47 × T_m).

2. Results and discussion

The alloy with a composition of Al-2.04at%Zn-1.37at%Mg-0.04at%Zr (or well-known as Al-4.8wt%Zn-1.2wt%Mg-0.14wt%Zr) was processed by casting. The as-cast material was homogenized in air at 470 °C for 8 h, and then hot extruded at 380 °C. Then, disks with a diameter of 20 mm and a thickness of 1.4 mm were cut from the extruded rods for processing by high-pressure torsion (HPT). The HPT process is described in detail elsewhere[12]. Before HPT processing, the alloy was homogenized at 470 °C for 1 h and then

water-quenched to room temperature (RT). The disks were subjected to 10 revolutions of HPT at RT under a pressure of 6 GPa and at a rotation speed of 1 rpm.

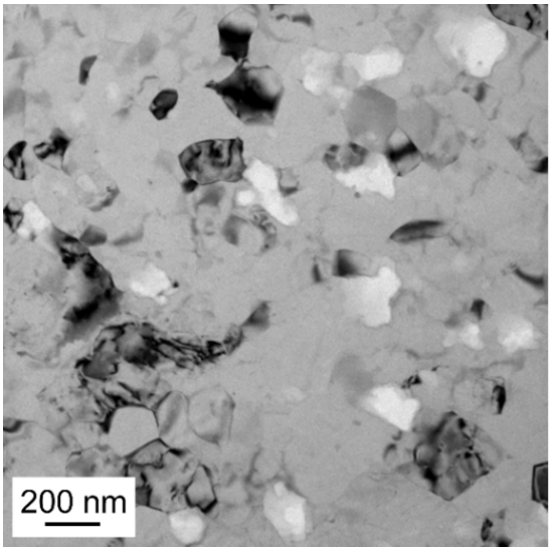

Fig. 1 Microstructure of the HPT-processed UFG Al-Zn-Mg-Zr alloy having an average grain size of ~ 200 nm.

As a result of HPT, a saturated UFG microstructure having an average grain size of 200 nm was produced, as shown in Fig. 1. Before performing tensile tests, the thermal stability and the strain rate sensitivity of the HPT-processed sample were studied in order to predict its ductility in the low temperature region between 120 and 170 °C. After annealing the HPT-processed sample for 2 hours at 120 °C, the average grain size was practically unchanged, and it increased only to about 300 nm at 170 °C, showing a stable UFG structure in this sample[13]. An unusually high strain rate sensitivity, m, of 0.43 ± 0.02 was obtained by using nanoindentation creep test in the same temperature region, indicating that superplasticity can be expected at low temperatures.

Samples were deformed by tension at different strain rates and different temperatures lower than 0.5 × T_m. Figure 2a shows the typical stress-strain curves of superplastic deformation taken at a strain rate of $\dot{\varepsilon} = 5 \times 10^{-4}\ s^{-1}$ at 120, 150 and 170 °C. It can be seen that a total elongation of almost 200% is obtained at a very low temperature of 120 °C (~0.42 × T_m), and a record deformation higher than 500% was observed at 170 °C (~0.47 × T_m).

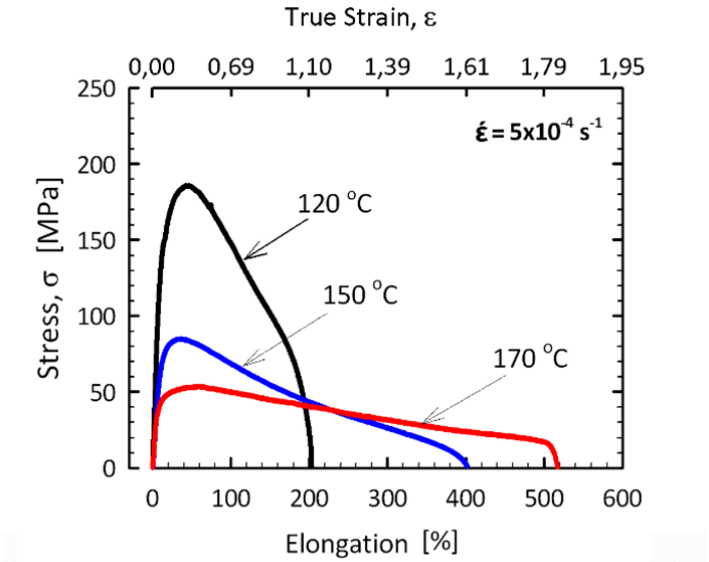

Fig. 2 Characteristics of low-temperature superplasticity in the UFG Al-Zn-Mg-Zr alloy. **(a)** Stress-strain (σ – ε) curves, showing a total elongation higher than 500%, **(b)** Logarithm of the stress (lnσ) obtained at elongation of 100% versus the reciprocal of testing temperature (1/T) for the determination of the activation energy (Q) of the deformation process.

To analyze the experimental results, the activation energy, Q, of the deformation process, characterizing the superplastic flow can be determined by using equations (1-2) in another form:

$$\dot{\varepsilon} = B \cdot \sigma^{1/m} \cdot exp\left(\frac{-Q}{RT}\right), \quad (3)$$

which describes the stress- and temperature-dependence of the strain rate. In equation (3), B is a constant depending on the properties of material. Taking the stress values at the same

elongation of 100% ($\varepsilon = 0.69$) for different testing temperatures, using the value of 0.43 for m obtained by indentation creep, from the slope of the $\ln\sigma - 1/T$ line, a value of 68 kJ/mole can be estimated for the activation energy, Q (see Fig. 2b). Considering both the high strain rate sensitivity and the relative stability of the microstructure of the sample during deformation, the basic mechanism of the superplastic deformation of the investigated UFG alloy should certainly be grain boundary sliding. The experimentally determined activation energy of 68 kJ/mole is lower than the values for self-diffusion in Al (142 kJ/mole)[14] or grain boundary diffusion in Al (84 kJ/mole)[14]. In order to explain the occurrence and significance of the experimentally obtained activation energy, let us examine the microstructure of the superplastically deformed samples.

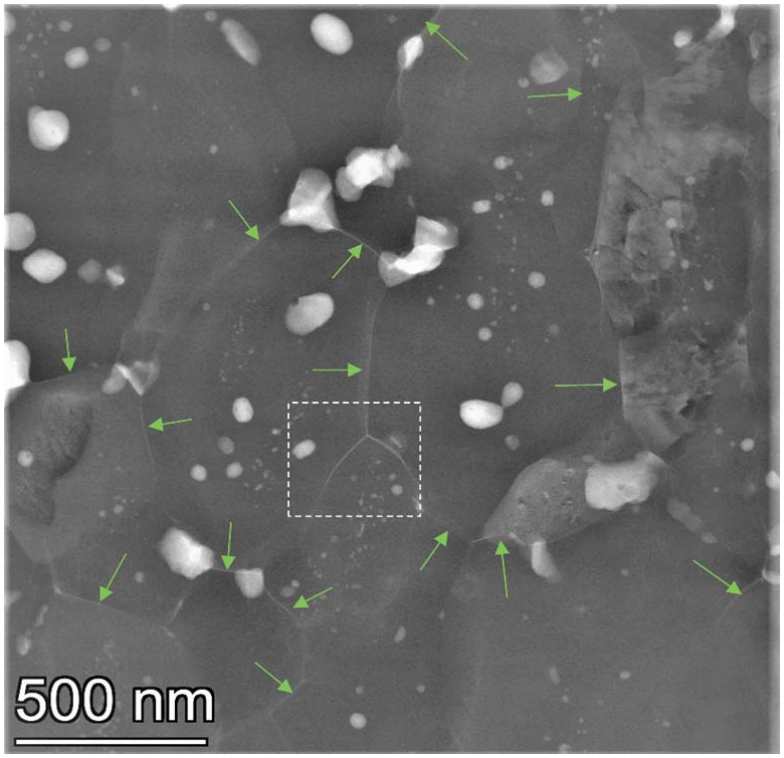

Fig. 3 Microstructure of the deformed samples. Low magnification STEM-HAADF image for the sample superplastically deformed at 170 °C and a strain rate of 5×10^{-4} s^{-1}, showing the existence of Zn-containing particles (bright ones) and Zn-rich Al/Al grain boundaries (indicated by the green arrows).

Figure 3 shows a HAADF image obtained by STEM on the sample deformed superplastically for a total elongation higher than 500% at 170 °C. Besides the $MgZn_2$ phase particles, which appear as bright areas on the image since the atomic number of Zn is much higher than that of Al, Zn-rich Al/Al grain boundaries indicated by small green arrows can also be observed. A small area of the image marked with a white dashed square is shown with a higher magnification in Fig. 4a and analyzed by using energy-dispersive X-ray spectroscopy (EDS) mapping in Figs. 4b-e.

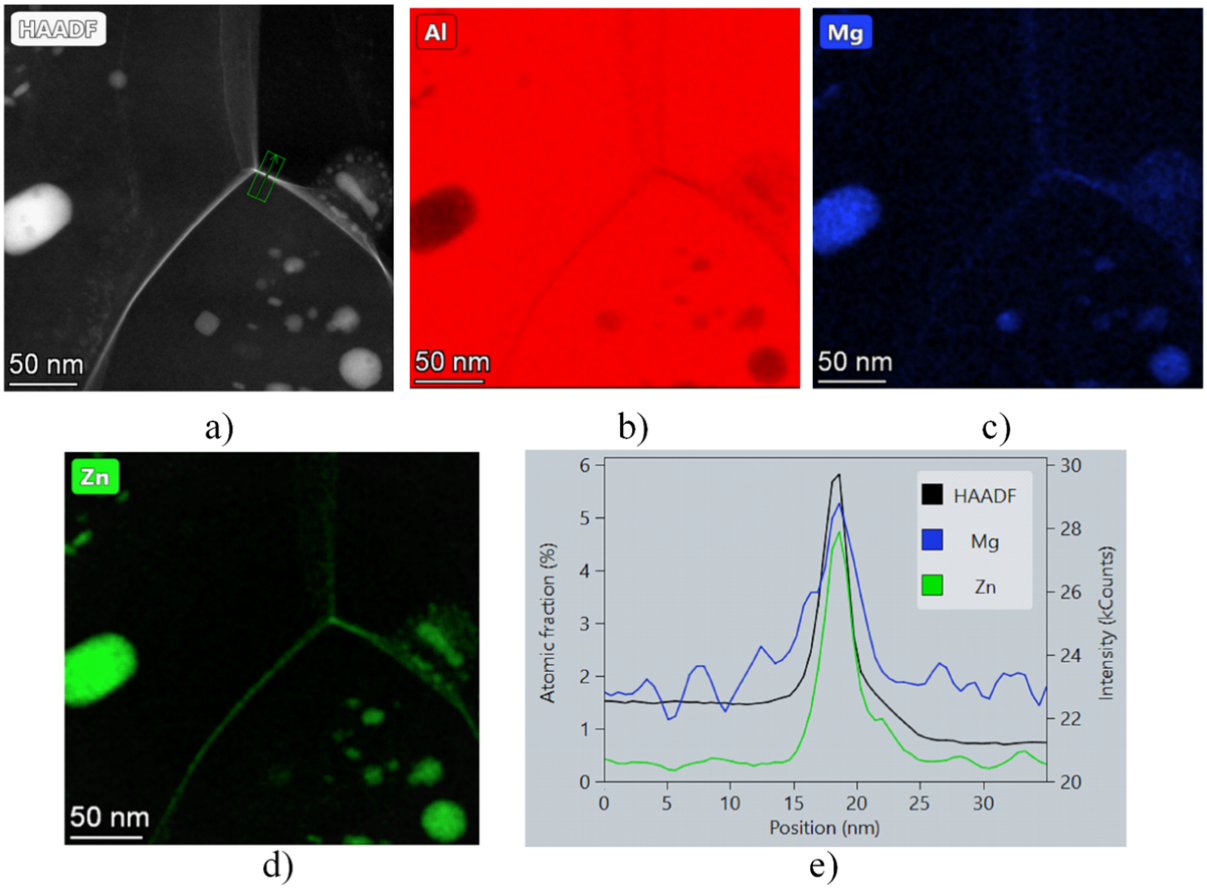

Fig. 4 High magnification STEM results. (**a)** HAADF image showing Zn-rich grain boundaries (forming a brightly imaged triple junction, (**b-d)** corresponding EDS maps for Al, Mg and Zn, respectively, (**e)** EDS line profile analysis along a boundary, marked by arrows in the HAADF image, showing the segregation of Zn and Mg atoms into Al/Al grain boundaries in the HPT-processed UFG sample.

The EDS results reveal clearly the depletion of Al (see Fig. 4b), and the excess of Mg and Zn atoms (shown in Figs. 4c and 4d, respectively) in the Al/Al grain boundaries of this HPT-processed UFG sample. EDS measurements at different locations also show that the fractions of Zn and Mg change along the grain boundaries and there are places where Zn atoms are the main contributors to the excess solute atoms in the Al/Al grain boundaries, while in other locations the concentration of Mg is higher than that of Zn. Nevertheless, the matrix grain boundaries of this UFG sample can be regarded as Zn/Mg-rich boundaries. For instance, Fig. 4e reveals that the sum of Zn and Mg concentrations in the boundary reached about 10 at.%.

The segregation of solute atoms to the grain boundaries in an HPT-processed supersaturated solid solution was recently interpreted by numerical and analytical calculations[15]. During the SPD process, after reaching a saturated UFG microstructure, the role of the grain boundaries is enhanced in subsequent deformation processes due to the significance of grain boundary sliding[3,9,16]. It was shown in the mentioned numerical calculations that GBS can relax the external shear stress during SPD, forming an inhomogeneous stress field around the sliding grain boundaries[15]. The hydrostatic component (p) of this stress field may induce up-hill diffusion currents, leading to accumulation sites for both vacancies and solute atoms at the grain boundaries. It should be noted that the mentioned hydrostatic component causes different currents for different volume-size solute atoms. According to the theoretical calculation, Fig. 5 shows an example demonstrating the trapping effect of a sliding boundary for larger (e.g., Mg) and smaller (e.g., Zn) solute atoms (compared to the Al matrix) at the opposite sides of the sliding grain boundary. Considering the EDS line profiles for Zn and Mg shown in Fig. 4e, the segregation of the solute atoms with different sizes along the grain boundary seems to be experimentally confirmed.

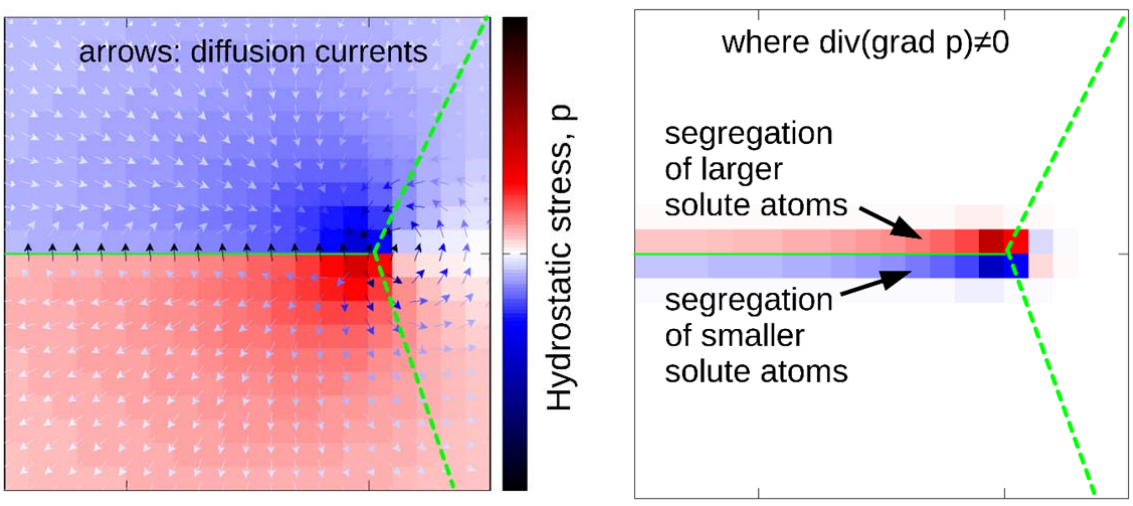

a) b)

Fig. 5 Trapping effect of sliding grain boundary. (a) Calculated hydrostatic stress component (p) around a slipped grain boundary (the arrows show the direction of the negative stress gradient, and then the diffusion currents), **(b)** Accumulation points for solute atoms smaller (red) and larger (blue) than the matrix atoms (Al). The green dashed lines represent the grain boundaries.

The strong segregation of Zn to the matrix grain boundaries is already a known phenomenon in high-Zn concentrated binary Al-Zn alloys with a UFG structure[17–19], but it has not been reported yet for the 7xxx series Al alloys. This is a key point in the observed low-temperature superplasticity for the present UFG Al-Zn-Mg-Zr alloy. Since superplasticity is based on grain boundary diffusion, it is worth to calculate the diffusion coefficient, D, using the formula (2). For grain boundary diffusion in both pure Al and Zn, the values of D_0 are similar and lie between ~1.3×10^{-14} and ~5×10^{-14} m^2 s^{-1} as shown in a previous study[14]. Using the activation energy of Q = 84 kJ/mole for grain boundary diffusion of Al at T = 443 K (corresponding to 170 °C)[14], it follows that the diffusion coefficient, D, may be estimated to be between 1.60×10^{-24} and 6.16×10^{-24} m^2 s^{-1}. Applying the experimentally determined

activation energy of 68 kJ/mole, the value of D can be found between 1.23×10^{-22} and 4.74×10^{-22} m^2 s^{-1} at 170 °C, which is almost two orders of magnitude higher than the aforementioned values calculated for grain boundary diffusion in Al.

We can claim that it is Zn segregation at the grain boundaries that contributes to the enhanced diffusion at grain boundaries. Indeed, according to both experimental and simulation results shown in Figures 3, 4 and 5, respectively, the HPT-processed Al-Zn-Mg-Zr sample can be regarded as a two-phase system comprising a grain interior phase and a thin layer grain boundary phase enriched in Zn and Mg. Considering the Al-Zn binary phase diagram, the addition of Zn to Al yields a lower temperature of melting. Similar effect can be observed when Mg is added to Al. For relatively low Zn and Mg concentrations, 1 at.% solute addition results in a reduction of the solidus temperature with 8.3 and 13 K, respectively. The solidus temperature can be considered as a quasi-melting point of the grain boundary phase. Thus, for the grain boundary composition shown in Fig. 4e, the concentrations of Zn and Mg (4 and 6 at.%, respectively) can cause more than 100 K reduction of the melting point. Due to the lower melting point, the testing temperatures between 120 and 170 °C corresponded to an elevated homologous temperature higher than 0.5 during deformation with GBS. Indeed, for fcc crystals the activation energy of grain boundary diffusion is proportional with the melting point and the proportionality constant is 0.078 kJ/(mole·K)[20]. Using the estimated melting point of the grain boundary phase (about 830 K), 65 kJ/mole is calculated for the activation energy of grain boundary diffusion which agrees with the measured value within the experimental error (68 ± 5 kJ/mole). The higher quasi-homologous temperature is certainly an important factor which resulted in a higher activation of grain boundary sliding and thereby contributed highly to the excellent superplasticity. As noted above, in the UFG Al-Zn alloy an enhanced GBS and a high ductility are observed even during deformation at RT.

Considering separately the segregation of Zn and Mg solutes to grain boundaries, it should be noted that both the experimental results (see Fig. 4e) and recent simulations and

theoretical calculations reveal a significant difference between the profiles of these atoms across the grain boundary[21]. While a relatively broad segregation having 5–6 nm half-width can be observed for Mg, a much thinner Zn layer with 2–3 nm half-width formed at the boundary shown in Figure 3. This is due to the extra effect of the electronic structure in the case of Zn, as 3d element[21]. Because of the broad segregation, the promoting effect of Mg addition on the deformation in the grain boundaries due to the reduction of the quasi-melting point can be lowered or even suppressed by the hindering effect of the large Mg atoms on the dislocation motion. Dislocation glide acts as a complementary mechanism beside grain boundary diffusion during superplastic deformation since the change of the grain shape can occur with the help of dislocation slip. Therefore, the broadly distributed Mg atoms with large size hinder the dislocation motion effectively in the vicinity of grain boundaries, thereby hindering the occurrence of superplastic deformation. Indeed, superplasticity has not been observed in ultrafine-grained Al-Mg solid solutions without Zn addition. If the effect of Mg on the melting point depression in the grain boundaries is neglected, the Zn segregation alone yields a grain boundary activation energy of about 70 kJ/mole (see the previous paragraph for the fundamentals of this calculation) which is also close to the experimentally determined activation energy of the superplastic deformation for the present alloy (68 kJ/mole). Thus, it is the grain boundary segregation of Zn, rather than Mg, that is responsible for the accelerated diffusion and enhanced sliding, which are necessary conditions for the occurrence of superplasticity at lower temperatures. It is also evident that the increased concentration of defects (vacancies and grain boundary dislocations) at grain boundaries in UFG alloys may also make a certain contribution to the acceleration of these processes[15,22,23]. Furthermore, the presence of Zn particles in triple junctions may contribute to the steadiness of the superplastic flow process[24].

The significant advantage of low-temperature superplasticity is, on the one hand, the potential energy savings during low temperature deformation, and on the other hand, the

preservation of the fine-grained microstructure. Experimental results have shown that, as it can be seen in Fig. 3, the microstructure of the sample after superplastic deformation at 170 °C remains equiaxial and ultrafine with an average grain size of about 400 nm. Similarly to the effect of static annealing, $MgZn_2$ phase small precipitates with a size between 10 and 70 nm were formed inside the grains during deformation at 170 °C. Owing to both the ultrafine grain size and the strengthening particles, the material retains its high strength even after superplastic deformation, as shown in Fig. 6, where the room temperature Vickers hardness (HV) of the HPT-processed and the superplastically deformed UFG samples can be seen and compared with the peak hardness of the initial coarse-grained sample.

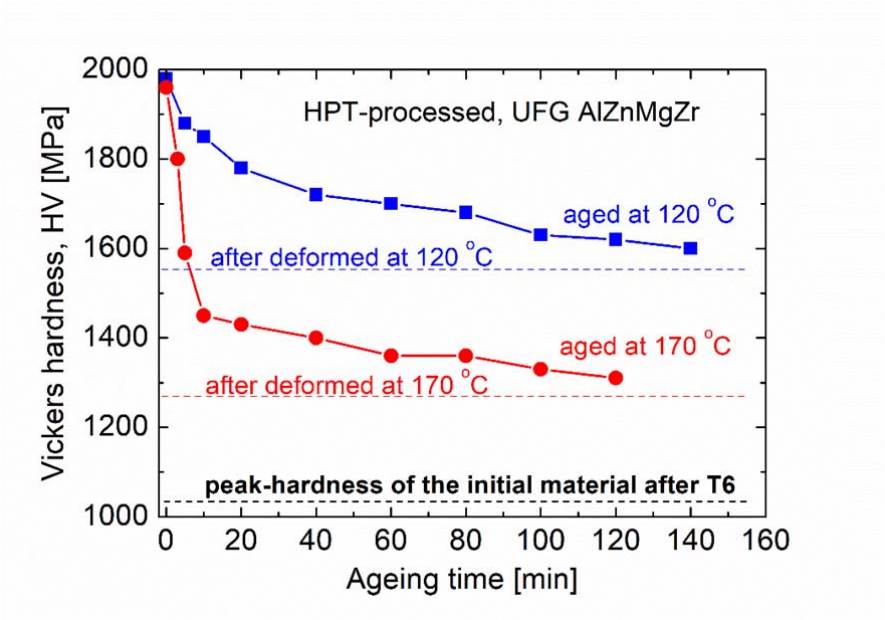

Fig. 6 Results on Vickers hardness. The room temperature Vickers hardness (HV) of the samples after superplastic deformation at 120 °C (blue dashed line) and 170 °C (red dashed line), as well as the peak hardness obtained for the initial coarse-grained sample after the conventional T6 treatment (black dashed line). The hardness values of the HPT-processed UFG samples statically annealed for different times at 120 °C (blue solid square) and 170 °C (red solid circle) are also plotted to show the thermal stability of this sample.

It is well established that the so-called T6 conventional heat treatment must be applied to the 7xxx series alloys for producing the maximum strength[25,26]. This treatment conventionally includes the aging at 120 °C for 24 hours of quenched and supersaturated samples, resulting in the maximum strengthening effect of precipitates. In the present case, the peak hardness of the initial sample after the T6 treatment is ~1020 MPa. It can be seen that the hardness values of the samples after superplastic deformation (1280 and 1560 MPa at 170 and 120 °C, respectively) are still 20-50% higher than the mentioned peak hardness of the initial sample after the conventional T6 treatment. It should be noted that without annealing the hardness of the HPT-processed UFG sample (~1960 MPa) is almost double the mentioned peak hardness of the initial coarse-grained sample, unambiguously confirming the significance of SPD processing. When annealing is implemented at temperatures not higher than 170 °C, together with some activated effects decreasing the hardness, the microstructure of the HPT-processed sample remains relatively stable, preserving the high strength.

Summarizing the above, the performed research demonstrates for the very first time the possibility of extremely low-temperature superplasticity in traditional Al alloys of the 7xxx series. The origin of this effect is related to the formation, through SPD processing, of an UFG structure where Zn segregations are present at grain boundaries, providing accelerated diffusion and enhanced sliding at lower temperatures. The discovery of the low-temperature superplasticity creates an opportunity for the development of new technologies for the superplastic forming of complex-shaped products exhibiting a high structural strength in operating conditions at room temperature.

Methods

HPT processing. The HPT process is described in detail elsewhere[12].

Microstructural studies. The microstructure of the HPT-processed sample was investigated by transmission electron microscopy (TEM). First, a thin foil was prepared by mechanical polishing and then it was thinned till perforation at -20 °C by twin-jet electropolishing using a chemical solution containing 33% HNO3 and 67% CH3OH. A Titan Themis G2 200 scanning transmission electron microscope (STEM) was used for TEM and energy-disperse X-ray spectroscopy (EDS) investigations. The microscope was equipped with a four-segment Super-X EDS detector. A corrector for the spherical aberration (Cs) was applied at the imaging part, while no probe-correction was present. The STEM images were taken by a Fishione high-angle annular dark-field (HAADF) detector. The elemental maps were recorded by EDS in spectrum-image mode.

Strain rate sensitivity tests. Strain rate sensitivity of the investigated samples were determined by indentation creep carried out in the temperature range of 100÷170 ^{o}C using a Nanoindenter G200 machine working with maximum load of 50 mN and a three-sided, customized Berkovich pyramid. Elevated testing temperatures were realized using a commercial heating stage (MTS Nanoinstrument). The procedure for determination of strain rate sensitivity by using indentation creep can be found in Ref.[27].

Tensile tests. Samples with a gauge length of 2.0 mm and a cross section of 1.0 × 0.8 mm were fabricated from the HPT-processed disk and deformed by tension at different strain rates and different temperatures lower than 0.5 × T_m. Tensile tests were conducted at testing temperature of 120, 150, 170 °C and strain rate $\dot{\varepsilon}$ of 5×10^{-4} s^{-1} by using the testing machine Instron 5982. Vickers microhardness was measured using a Zwick Roell ZHμ hardness tester with a load of 5 N for dwell time of 10 s.

Data availability

The data that support the findings of this study are all own results of the authors, not available anywhere.

References

[1] Nich, T. G., Wadsworth, J. & Sherby, O. D. *Superplasticity in Metals and Ceramics* (Cambridge University Press, Cambridge, 1997).

[2] Langdon, T. G. Seventy-five years of superplasticity: historic developments and new opportunities. *J. Mater. Sci.* **44,** 5998-6010 (2009).

[3] Valiev, R. Nanostructuring of metals by severe plastic deformation for advanced properties. *Nature Mater.* **3,** 511-516 (2004).

[4] Valiev, R. Z., Estrin, Yu., Horita, Z., Langdon, T. G., Zehetbauer, M. J. & Zhu, Y. T. Producing bulk ultrafine-grained materials by severe plastic deformation. *JOM* **58(4),** 33-39 (2006).

[5] Kaibyshev, O. A. *Superplasticity of Alloys, Intermetallides and Ceramics* (Springer-Verlag Berlin, Heidelberg, 1992).

[6] Kawasaki, M. & Langdon, T. G. Review: Achieving superplastic properties in ultrafine-grained materials at high temperatures. *J. Mater. Sci.* **51,** 19-32 (2016).

[7] McFadden, S. X., Mishra, R. S., Valiev, R. Z., Zhilyaev, A. P. & Mukherjee, A. K. Low-temperature superplasticity in nanostructured nickel and metal alloys. *Nature* **398**, 684-686 (1999).

[8] Ovid'ko, I.A., Valiev, R. Z. & Zhu, Y. T. Review on superior strength and enhanced ductility of metallic nanomaterials. *Prog. Mater. Sci.* **94,** 462-540 (2018).

[9] Liu, F. C. & Ma, Z. Y. Contribution of grain boundary sliding in low-temperature superplasticity of ultrafine-grained aluminum alloys. *Scripta Mater.* **62**, 125-128 (2010).

[10] Sauvage, X., Wilde, G., Divinski, S. V., Horita, Z. & Valiev, R. Z. Grain boundaries in ultrafine grained materials processed by severe plastic deformation and related phenomena. *Mater. Sci. Eng. A* **540,** 1-12 (2012).

[11] Zhang, Y. D., et al. Dynamic precipitation, segregation and strengthening of an Al-Zn-Mg-Cu alloy (AA7075) processed by high-pressure torsion. *Acta Mater.* **162,** 19-32 (2019).

[12] Valiev, R.Z., Zhilyaev A. P. & Langdon, T. G. *Bulk Nanostructured Materials: Fundamentals and Applications* (John Wiley & Sons, Inc., Hoboken, New Jersey, 2013).

[13] Gubicza, J., et al. Evolution of microstructure and hardness during artificial aging of an ultrafine-grained Al-Zn-Mg-Zr alloy processed by high pressure torsion. *J. Mater. Sci.* **55**, 16791-16815 (2020).

[14] Frost, H. J. & Ashby, M. F. *Deformation-Mechanism Maps: The Plasticity and Creep of Metals and Ceramics* (Pergamon Press, Oxford, 1982).

[15] Kovács, Zs. & Chinh, N. Q. Up-hill diffusion of solute atoms towards slipped grain boundaries: A possible reason of decomposition due to severe plastic deformation. *Scripta Mater.* **188**, 285-289 (2020).

[16] Chinh, N. Q., Szommer, P., Horita, Z. & Langdon, T. G. Experimental evidence for grain boundary sliding in ultrafine-grained aluminum processed by severe plastic deformation. *Adv. Mater.* **18**, 34-39 (2006).

[17] Valiev, R. Z., et al. Unusual super-ductility at room temperature in an ultrafine-grained aluminum alloy. *J. Mater. Sci.* **45,** 4718-4724 (2010).

[18] Straumal, B., et al. Thermal evolution and grain boundary phase transformations in severely deformed nanograined Al-Zn alloys. *Acta Mater.* **56,** 6123-6131 (2008).

[19] Edalati, K., Horita, Z. & Valiev, R. Z. Transition from poor ductility to room-temperature superplasticity in a nanostructured aluminum alloy. *Scientific Reports* **8,** 6740 (2018).

[20] Gubicza, J. *Defect Structure and Properties of Nanomaterials* (Woodhead Publishing, Duxford, 2017).

[21] Petrik, M. V., Kuznetsov, A. R., Enikeev, N. A., Gornostyrev, Yu. N. & Valiev, R. Z. Peculiarities of interactions of alloying elements with grain boundaries and the formation of segregations in Al-Mg and Al-Zn alloys. *Phys. Met. Metallogr.* **119**, 607-612 (2018).

[22] Kwiecinski, J. & Wyrzykowski, J. W. Investigation of grain boundary self-diffusion at low temperatures in polycrystalline aluminium by means of the dislocation spreading method. *Acta Metall. Mater.* **39**, 1953-1958 (1991).

[23] Kolobov, Yu. R., et al. *Grain Boundary Diffusion and Properties of Nanostructured Materials* (CISP: Cambridge International Science Publishing, Cambridge, 2007).

[24] Bobruk, E. V., Sauvage, X., Enikeev, N. A. & Valiev, R. Z. Influence of fine scale features on room temperature superplastic behavior of an ultrafine-grained Al-30Zn alloy. *Mater. Lett.* **254,** 329-331 (2019).

[25] Polmear, I. J. *Light Alloys-Metallurgy of the Light Metals*, *3rd ed.* (Arnold, London, 1995).

[26] Azarniya, A., Taheri, A. K. & Taheri, K. K. Recent advances in ageing of 7xxx series aluminum alloys: a physical metallurgy perspective. *J. Alloys Compd*. **781**, 945- 983 (2019).

[27] Chinh, N. Q. & Szommer, P. Mathematical description of indentation creep and its application for the determination of strain rate sensitivity. *Mater. Sci. Eng. A* **611**, 333-336 (2014).

Acknowledgements

This research was supported by the Hungarian-Russian bilateral Research program (TÉT) No. 2017-2.3.4-TÉT-RU-2017-00005. This work was completed in the ELTE Institutional Excellence Program (TKP2020-IKA-05) financed by the Hungarian Ministry of Human Capacities. R.Z.V. and M.Y.M. acknowledge the support in part from the Russian Foundation for Basic Research (project No. 20-03-00614) and in part from the Ministry of Science and Higher Education of the Russian Federation under grant agreement No. 0838-2020-0006.

Author contributions

N.Q.C. and R.Z.V. conceived and guided the research. M.Y.M. and E.V.B. implemented the HPT processing and tensile tests. J.L.L. and J.G. performed the structural studies. Zs.K. carried out the simulation calculations. A.Q.A. and V.M.K. conducted the indentation and hardness tests. N.Q.C., R.Z.V., M.Y.M., J.G. and Zs.K. interpreted and discussed the results, and wrote the text of the paper.

Competing interests

The authors declare no competing interests.

Materials & Correspondence:

Nguyen Q. Chinh, email: chinh@metal.elte.hu

Ruslan Z. Valiev, email: ruslan.valiev@ugatu.su